

Introduction

The location information of a User Equipment (UE) is essential for many applications, e.g. emergency services, autonomous driving, intelligent transportation systems, 6G networks.

Global Navigation Satellite Systems perform poorly in **urban environments**, where the likelihood of line-of-sight (LOS) conditions is low. Hence, alternative approaches, which are **robust to non-LOS** conditions are required.

We present **LocUNet^a**: A deep learning method for localization, based on **Received Signal Strengths (RSS)** of the beacon signals of Base Stations (BSs)^b at the UE to be localized, and the corresponding pathloss (for known BS power, pathloss is deducible from RSS, and vice versa) radio map estimates (via recently proposed **RadioUNet[2]**) of the area of interest for each BS.

Reporting **RSS** information is a **standard feature** in most of the current wireless protocols and **does not require any further specific hardware at the UE**, whereas the time-based (ToA and TDoA) and angle-based (AoA) methods require high precision clocks and antenna arrays, respectively.

Two Novel Datasets For Urban Positioning

Prepared using WinProp [3], publicly available for the research community to investigate the performances of RSS and ToA ranging-based localization algorithms (See [1] for details).

- **RadioLocSeer**: Simulated and estimated (via RadioUNet [2]) pathloss radio maps under different simulation models (*Dominant Path Model* (DPM) and *Intelligent Ray-Tracing with 2 Interactions* (IRT2)), along with the corresponding buildings, cars, BSs, and roads in image format. UE (200 per map) and well-separated BS locations (5 per map) are provided, as well.
- **RadioToASeer**: Dataset of the ToA values of the same maps of RadioLocSeer based on DPM, i.e., ToA values for potential UE locations are found based on the dominant ray (i.e., the multi-path-component with the highest energy, which is the ray with shortest free space path) that propagates from the BS to the UE location. Using this dataset serves as quasi-lower bounds for the errors of the ToA ranging-based methods.

LocUNet Scenarios

We present three different scenarios to showcase the performance of LocUNet (and the compared algorithms) under different degrees of accuracy of the radio map estimate (input feature for LocUNet), with respect to the true radio map, from which the pathloss measurements are taken. We use two different simulation methods (DPM and IRT) to represent the potential discrepancy between the real wave propagation phenomena and the model used to estimate the radio maps.

1. **DPM**: In this very optimistic scenario, we assume that the real radio maps are exactly governed by DPM and the radio map estimates are obtained by RadioUNet, which was trained in supervised fashion to estimate radio maps also under the DPM assumption. Hence, LocUNet enjoys having access to very high accuracy radio maps, where the inaccuracy of the available radio maps with respect to true radio maps is solely due to the prediction error of RadioUNet.
2. **DPMTolRT2**: Different from the previous scenario, here, the pathloss measurements stem from IRT2 simulations, while the radio map estimations are obtained from RadioUNet (trained for DPM), as before.
3. **DPMTolRT2Cars**: Similar setting as in DPMTolRT2, but the pathloss measurements stem from IRT2 simulations for an environment with additional obstructions (cars), unknown to LocUNet. This scenario encompasses all the important sources of mismatch between the radio map estimates and the true real maps.

^aLonger version of this work is available at [1].

^bEssentially, any wireless signal source with known location, e.g., WiFi-Hot-spots, can be utilized.

Structure of LocUNet

A **UNet variant**, with the final layer of **center of mass (CoM)** (μ_x, μ_y) of output $H(x, y)$ of the previous layer (*quasi-heatmap*, as it admits negative values due to the LeakyReLU being the activation function),

$$\mu_x = \frac{\sum_{x=1}^{256} \sum_{y=1}^{256} xH(x, y)}{\sum_{x=1}^{256} \sum_{y=1}^{256} H(x, y)}, \quad \mu_y = \frac{\sum_{x=1}^{256} \sum_{y=1}^{256} yH(x, y)}{\sum_{x=1}^{256} \sum_{y=1}^{256} H(x, y)},$$

where 256 is the number of pixels along each axis.

LocUNet takes pathloss measurements and radio map estimations for each BS as inputs (optionally, the map of the buildings and the BS positions as one-hot images) and falls into the category of *spatial regression* approach with respect to previous localization works in image processing (cf. [1] for a detailed overview).

An Example

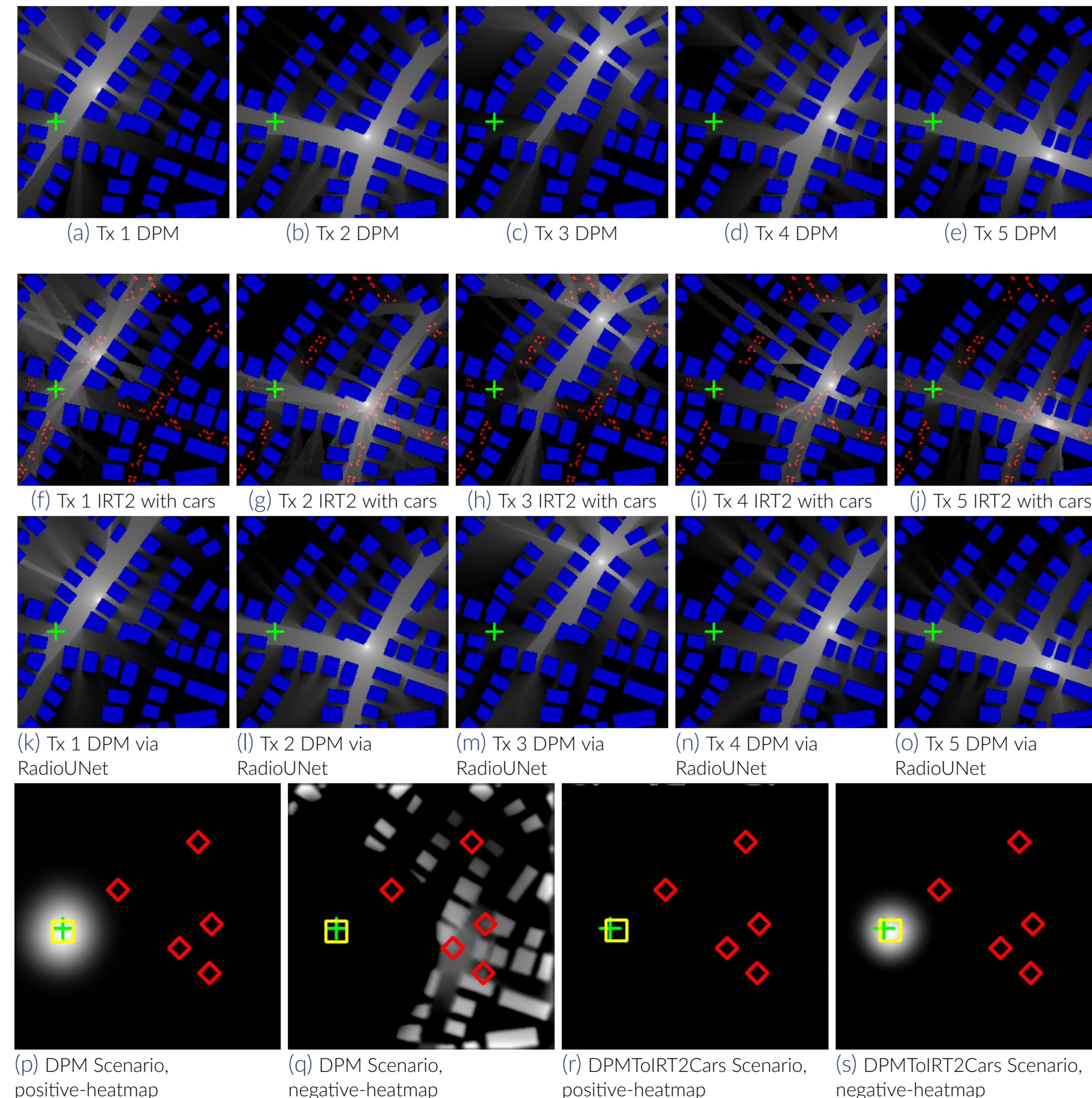


Figure 1. A generic localization problem from RadioLocSeer Dataset, where the pathloss at the UE from each BS is moderate. **First row**: DPM true radio maps. **Second row**: IRT with cars true radio maps. **Third row**: DPM estimated maps by RadioUNet. **Fourth row**: LocUNet results for the scenarios DPM and DPMTolRT2Cars. We call the positive and the negative part of the quasi-heatmap positive-heatmap and negative-heatmap. The normalized positive (by max. pixel value) and the negative (by min. pixel value) heatmaps of LocUNet before CoM layer are shown in gray-level. Buildings are blue, Tx locations are marked with red diamonds. Estimated and true locations are marked with yellow square and green cross, respectively.

Numerical Results

Table 1. Comparison with fingerprint-based methods using the RadioLocSeer Dataset for the scenarios described. Accuracies are in **mean absolute value (MAE)**, which is the average 2D Euclidean distance between the estimated UE location and the ground-truth location, in unit of meters.

Algorithm	DPM	DPMTolRT2	DPMTolRT2Cars	(ms)
kNN [4]	7.01	23.38	27.19	~ 20
Adaptive kNN [5]	7.49	25.39	29.51	~ 20
LocUNet	4.73	9.48	13.15	~ 5

Table 2. Comparison with ToA ranging-based methods using the RadioToASeer Dataset.

Algorithm	MAE (ms)
POCS [6, 7]	37.89 ~ 15
SDP [8]	7.16 ~ 600
Robust SDP 1 [9]	7.55 ~ 600
Robust SDP 2 [10]	7.63 ~ 600
Bisection-based robust method [11]	9.49 ~ 16
Max. correntropy criterion method [12]	12.45 ~ 30
LocUNet DPM	4.73 ~ 5

Summary

- Thanks to its fully-convolutional design, **LocUNet** effectively utilizes (cf. [1]) radio map estimates to achieve **state-of-the-art localization performance** and enjoys **high robustness to inaccuracies** of these input radio maps w.r.t. the actual radio maps.
- The proposed method does not require pre-sampling of the environment; and is suitable for real-time applications, thanks to the **RadioUNet[2]**, a neural network-based radio map estimator, which can very accurately **approximate ray-tracing** simulations, but **much faster**.
- We provide two simulated **novel datasets** in the urban setting to promote **realistic assessments of performances of RSS fingerprint and ToA ranging-based algorithms**. We hope that researchers will benefit from our datasets to benchmark their proposed methods in realistic urban setting.
- To the best of our knowledge, this is the **first work in the literature to provide numerical comparisons among numerous RSS fingerprinting and ToA ranging-based methods in a realistic urban setting**.

References

- [1] C. Yapar, R. Levie, G. Kutyniok, and G. Caire, "Real-time outdoor localization using radio maps: A deep learning approach," p. arXiv:2106.12556, 2021.
- [2] R. Levie, C. Yapar, G. Kutyniok, and G. Caire, "RadioUNet: Fast radio map estimation with convolutional neural networks," *IEEE Transactions on Wireless Communications*, vol. 20, no. 6, pp. 4001–4015, 2021.
- [3] R. Hoppe, G. Wölfe, and U. Jakobus, "Wave propagation and radio network planning software WinProp added to the electromagnetic solver package FEKO," in *Proc. Int. Appl. Computational Electromagnetics Society Symp. - Italy (ACES)*, Florence, Italy, March 2017, pp. 1–2.
- [4] P. Bahl and V. N. Padmanabhan, "RADAR: An in-building RF-based user location and tracking system," in *Proceedings IEEE INFOCOM 2000. Conference on Computer Communications. Nineteenth Annual Joint Conference of the IEEE Computer and Communications Societies*, 2000, vol. 2, pp. 775–784 vol.2.
- [5] J. Oh and J. Kim, "Adaptive k-nearest neighbour algorithm for WiFi fingerprint positioning," *ICT Express*, vol. 4, no. 2, pp. 91–94, 2018, SI on Artificial Intelligence and Machine Learning.
- [6] A. O. Hero and D. Blatt, "Sensor network source localization via projection onto convex sets (POCS)," in *Proceedings. (ICASSP 05). IEEE International Conference on Acoustics, Speech, and Signal Processing, 2005.*, 2005, vol. 3, pp. iii/689–iii/692 Vol. 3.
- [7] M. R. Gholami, H. Wymeersch, E. G. Ström, and M. Rydström, "Wireless network positioning as a convex feasibility problem," *EURASIP Journal on Wireless Communications and Networking*, vol. 2011, no. 1, pp. 161, 2011.
- [8] R. M. Vaghefi, J. Schloemann, and R. M. Buehrer, "NLOS mitigation in TOA-based localization using semidefinite programming," in *2013 10th Workshop on Positioning, Navigation and Communication (WPNC)*, Dresden, Germany, 2013, pp. 1–6.
- [9] G. Wang, H. Chen, Y. Li, and N. Ansari, "NLOS error mitigation for TOA-based localization via convex relaxation," *IEEE Transactions on Wireless Communications*, vol. 13, no. 8, pp. 4119–4131, 2014.
- [10] H. Chen, G. Wang, and N. Ansari, "Improved robust TOA-based localization via NLOS balancing parameter estimation," *IEEE Transactions on Vehicular Technology*, vol. 68, no. 6, pp. 6177–6181, 2019.
- [11] S. Tomic, M. Beko, R. Dinis, and P. Montezuma, "A robust bisection-based estimator for TOA-based target localization in NLOS environments," *IEEE Communications Letters*, vol. 21, no. 11, pp. 2488–2491, 2017.
- [12] W. Xiong, C. Schindelhauer, H. Cheung So, and Z. Wang, "Maximum correntropy criterion for robust TOA-based localization in NLOS environments," *arXiv e-prints*, p. arXiv:2009.06032, Sept. 2020.